

# Multiscale Modeling of Collagen Fibril in Bone at Various Crosslink Densities: An Insight into Its Deformation Mechanisms

S. M. Pradhan<sup>1</sup>, K. S. Katti<sup>1</sup> and D. R. Katti<sup>1</sup>

**Abstract:** Multiscale modeling of collagen fibril is carried out by incorporating the material properties of collagen obtained from steered molecular dynamics into the finite element model of collagen fibril with inclusion of crosslinks. The results indicate that the nonbonded interactions between collagen and mineral contribute to the significant enhancement of the elastic modulus of collagen fibril at all the crosslink densities in both the low strain and high strain regimes. The crosslinks are found to play an important role in the mechanical response of collagen fibril, the enhancement in elastic modulus ranging from 5-11% for various crosslink densities compared to the collagen fibril with no crosslinks. Further, two different mechanisms of fibril deformation are described based on the characteristic length of collagen fibril. The deformation mechanism is governed by the pullout between the ends of collagen molecules in the overlap zone, following the breaking of crosslinks, if the effective length is greater than the characteristic length. However, if the effective length is less than the characteristic length the deformation mechanism is influenced by the shearing between the staggered collagen molecules which are adjacent to each other.

**Keywords:** Collagen, multiscale modeling, fibril, mechanics.

## 1 Introduction

The collagen molecules are fibrous structural proteins found in abundance in the human body, constituting 85-95% of body proteins [Termine and Robey (1996)], and known for superior mechanical properties [Hulmes et al. (1995); Bozec and Horton (2005)]. The collagen molecules assemble to form a highly organized structure known as collagen fibril, which is the basic building unit of bone and collagen-rich tissues [Fratzl and Weinkamer (2007)]. The collagen molecules are long and cylindrical structures composed of a triple-helix formed by three polypeptide chains

---

<sup>1</sup> NDSU, ND, U.S.A.

[Ramachandran and Kartha (1955)], also known as  $\alpha$ -chains, measuring about 300 nanometers in length and 1.23 nanometers in diameter [Landis et al. (1993b)]. There are at least 27 different types of collagen molecules found in vertebrates [Bhattacharjee and Bansal (2005)] and fibrillar collagen accounts for only seven of all the known collagen types [Kadler et al. (1996); Hulmes (2002); Koch et al. (2003); Pace et al. (2003)]. Type I is the most abundant fibrillar collagen that is widely found in bone, skin, tendon, cornea, vasculature and lung etc. The diameter of collagen fibrils range from fifty to several-hundred nanometers [Nanci (1999); Gupta et al. (2006)] while their length is unknown because they merge with neighboring fibrils [Weiner and Wagner (1998)]. The collagen fibril consists of an array of collagen molecules arranged parallel to each other and staggered by 67 nm (i.e. D period) with respect to each other along the longitudinal axis [Hodge and Petruska (1963)]. The staggering of collagen molecules results in a banded pattern along the length of fibril consisting of an alternating overlap and hole-zones, which correspond to the regions of high and low electron densities respectively in X-ray diffraction [Hodge and Petruska (1963)] and visible as consecutive stripes in electron micrographs. Hole-zone is a region separating the ends of two collagen molecules (i.e. N-terminus and C-terminus) aligned along the longitudinal axis of collagen. The sizes of hole-zone and overlap zone are 27 and 40 nanometers respectively [Hodge and Petruska (1963); Landis et al. (1993b)]. The covalent crosslinks develop between adjacent collagen molecules with the maturation of tissues, in the overlap zone, near the ends of collagen. This crosslinking between the adjacent ends of the collagen molecule plays an important role in the mechanical property for fibril. In bone, hydroxyapatite ( $\text{Ca}_{10}(\text{PO}_4)_6(\text{OH})_2$ ) mineralizes in the hole zone into a plate-like structures, which grow in size along the axial direction of collagen molecule and sideways along channels [Nylen et al. (1960); Traub et al. (1989); Landis et al. (1993b); Landis (1995)]. The mineral in bone consists of various impurities such as carbonate, and constitutes a significant portion of bone-65% by weight [Eastoe and Eastoe (1954); Fisher and Termine (1985); Currey et al. (2001); Dorozhkin and Epple (2002); Olszta et al. (2003)] and 33-43% by volume [Currey (1990); Olszta et al. (2003)]. In bone, the mineral component is responsible for imparting the necessary stiffness, strength, and rigidity.

In the mineralized collagen fibril the (0001) surface of hydroxyapatite is oriented normal to the collagen molecule. In addition to (0001) surface, the electron diffraction studies show that the (10 $\bar{1}$ 0) surfaces of HAP are also well developed and are oriented approximately parallel to each other [Moradianoldak et al. (1991); Landis et al. (1993b); Landis et al. (1996)]. A molecular dynamics study of collagen-hydroxyapatite interface was first carried out by Katti and coworkers [Bhowmik et al. (2007b, 2009)] showing the presence of strong interactions at the interface

which significantly affects the mechanics of the collagen molecule. This work also showed the important role played by water in mediating the interactions between collagen and mineral [Bhowmik et al. (2007b)]. Similar behavior has also been shown by Katti and coworkers, in a number of other nanocomposites such as nacre and polymer clay nanocomposites, in which the mechanical behavior of organic material is enhanced by mineral proximity [Katti et al. (2005); Ghosh et al. (2007); Sikdar et al. (2008)]. The mineral surface shares a significant interfacial area with collagen molecules within the collagen fibril leading to the substantial hydroxyapatite-collagen interactions. The mechanics collagen in the proximity of (0001) and  $10\bar{1}0$  surfaces of hydroxyapatite and directional dependence of mineral-collagen interactions have been studied in detail by using molecular dynamics [Katti et al. (2010)]. The results of this study indicate that the mechanics of collagen pulled in different directions with respect to hydroxyapatite is significantly different. The role of the thickness of mineral on the mechanical properties of the collagen-hydroxyapatite interface has been carried out by Qin et al., suggesting that the tensile modulus of biomineral surface converges around 2 nanometer thickness of mineral [Qin et al. (2012)]. Other studies of collagen-hydroxyapatite system include molecular dynamics study [Dubey and Tomar (2009a, b); Dubey and Tomar (2010)], density functional study [Almora-Barrios and de Leeuw (2010)], and continuum micromechanics study [Hellmich et al. (2004); Fritsch et al. (2009)]. In addition to collagen-hydroxyapatite systems, there are a number of molecular dynamics studies investigating the mechanical properties of single collagen molecules [Lorenzo and Caffarena (2005); Buehler (2006a); Gautieri et al. (2009); Pradhan et al. (2011)] that show a wide variation of elastic modulus. The steered molecular dynamics study of full-length collagen molecule that investigates the mechanical response of the entire 300 nanometers length is carried out for the first time by Katti and coworkers [Pradhan et al. (2011)].

The molecular modeling study of collagen microfibrils has been carried out by number of researchers [Streeter and de Leeuw (2010); Tang et al. (2010); Gautieri et al. (2011); Streeter and de Leeuw (2011)]. The two dimensional coarse grain study of unmineralized and mineralized collagen microfibril has been carried out by Buehler [Buehler (2007, 2008)]. Most of the studies found in the current literature are limited to the investigation of microfibril, and the study of collagen fibril is very scarce. While the collagen fibrils in bone are mineralized, majority of these microfibril models are either unmineralized or do not include the effect of minerals proximity in the mechanics of collagen molecules. Many molecular dynamics studies indicate the important role of mineral proximity [Bhowmik et al. (2007b); Katti et al. (2010)]. Recently, we have carried out multiscale modeling of mineralized collagen fibril by combining molecular modeling with the contin-

uum description of the fibril microstructure [Pradhan et al. (2014)]. In this prior study, the mechanical response of collagen in proximity of mineral is evaluated using steered molecular dynamics and incorporated into the three-dimensional finite element model of collagen fibril in the small displacement regime and without crosslink behavior. In the current work, we present the results of our simulation in a larger displacement regime as well as the deformation response of collagen fibril under various crosslink densities.

## 2 Model Construction and Simulation details

### 2.1 Collagen fibril model construction

The key feature of this model is the multiscale model of collagen fibril that bridges molecular level properties with the continuum model of fibril. Molecular dynamics is used to simulate collagen-hydroxyapatite interactions at the molecular scale, and finite element method is used to model the mechanical response of fibril. At the molecular scale, the collagen is pulled in the proximity of mineral, and the absence of mineral proximity using steered molecular dynamics. These conditions correspond to the different mineral environments of collagen inside the collagen fibril. The two mineral surfaces used in this study include (0001), and (10 $\bar{1}$ 0). For the construction of collagen-hydroxyapatite models, the solvated collagen molecule (PDB ID: 1k6f) is brought in the proximity of mineral surface and geometrically optimized by energy minimization using conjugate gradient method. The temperature and pressure are brought to 300 K and 1.01 bar respectively in 100 K and 0.25 bar steps. The Langevin-Dynamics and Nose-Hoover piston method are used to maintain temperature and pressure [Feller et al. (1995)]. The simulations are carried out using NAMD [Phillips et al. (2005)] package and CHARMM [MacKerell et al. (1998)] force field. The force field parameters for hydroxyapatite are obtained from prior work [Bhowmik et al. (2007a)].

Molecular dynamics is a computational method used to model the atomic scale dynamics of a molecular system. In this method, each atom moves in many-body potentials of all the other atoms and Newton's second law of motion is integrated to obtain the evolution of position and velocity of particles over time. Newton's second law of motion is given by,

$$\frac{d^2\vec{r}_i}{dt^2} = \frac{\vec{F}_i}{m_i} \quad (1)$$

where  $\vec{r}_i$  is a position,  $m_i$  is mass and  $\vec{F}_i$  is a force acting on particle  $i$  in the direction of  $\vec{r}_i$ . The force  $F_i$  acting on a particle is obtained by computing gradient of total potential energy function  $U(\vec{r}_1, \vec{r}_2, \vec{r}_3, \dots, \vec{r}_N)$  with respect to current configuration

as follows

$$\vec{F}_i = -\frac{\partial}{\partial \vec{r}_i} U(\vec{r}_1, \vec{r}_2, \vec{r}_3, \dots, \vec{r}_N) \quad (2)$$

where N is the total number of particles. The accelerations of a particles obtained from equation (1) can be used along with equations of motion to predict future position and velocity of particles based on the initial positions and velocities. This is carried out in a series of small time steps. Due to the complexity of the potential function, finite difference algorithms such as the Verlet algorithm is used for integration. The potential function used in our work is the CHARMM force field.

Steered molecular dynamics (SMD) allows for application of force or velocity to atoms or groups of atoms in the molecular dynamics framework. In constant-velocity SMD, the harmonic potential is used to restrain an atom of protein or center of mass of the group of atoms to a point in space. The restrained atoms are called SMD atoms and the restraint can be considered as a dummy atom. The restraint point is then moved with a constant velocity in a particular direction. The restrained atoms will experience a pull proportional to their separation from the restraint, which will cause them to follow the restraint. Assuming single reaction coordinate  $x$ , the external potential applied to SMD atoms is given by

$$U = K(x - x_o)^2 \quad (3)$$

where K is the stiffness of restraint,  $x_o$  is the initial position of restraint, and  $x$  is the final position of restraint. The force exerted on SMD atoms is given by

$$F_x = K(x_o + vt - x) \quad (4)$$

where  $v$  is the constant velocity.

## 2.2 Evaluation of load-displacement response of collagen

For evaluating load-displacement response, the collagen molecule is fixed at one end, and extended using a harmonic spring, at pulling rate of  $0.00003 \text{ ps}^{-1}$  using steered molecular dynamics. The spring constants of  $4 \text{ kcal/mol/\AA}^2$  and  $0.1 \text{ kcal/mol/\AA}^2$  were used for short ( $\sim 8.5 \text{ nm}$  long) and full-length ( $\sim 290 \text{ nm}$  long) molecules respectively. In the proximity of mineral, the short collagen molecule is pulled parallel and perpendicular to the hydroxyapatite (10 $\bar{1}$ 0) and (0001) surfaces respectively. Steered molecular dynamics is also used to estimate the breaking stress between the end of collagen and mineral (0001) surface. The center of mass of collagen with N-telopeptide ends is pulled perpendicular to the mineral surface

using a pulling rate of  $0.00003 \text{ ps}^{-1}$  until the collagen and mineral are completely detached. The breaking stress of  $7.67 \text{ pN}/\text{\AA}^2$  is estimated from the peak force during the detachment of collagen and mineral.

The elastic modulus of collagen is estimated for the small displacement regime ( $\sim 7\%$ ). The deformation of collagen beyond 7% displacement is considered to be inelastic and represented using a piecewise linear description for finite element modeling. For the collagen molecule, the elastic modulus is computed for a small displacement of 7% using a relation  $E = k \times L/A$ , where 'k' is the stiffness of load-displacement response, 'L' is the length of the collagen molecule, and 'A' denotes the cross-sectional area of collagen. The cross-sectional area of collagen is estimated by enclosing the Van der Waals surface of collagen with a cylinder, similar to the method used by other researchers [Lorenzo and Caffarena (2005); Gautieri et al. (2009)]. The modulus of collagen in absence of mineral proximity is 2.95 GPa, whereas moduli for collagen molecule pulled parallel to  $(10\bar{1}0)$  and perpendicular to mineral  $(0001)$  surfaces are 13.17 and 6.26 GPa respectively [Pradhan et al. (2014)].

### ***2.3 Collagen-collagen and collagen-mineral interface and development of finite element model***

The collagen-collagen interface and collagen-mineral interface are assumed to consist of a thin region called "interlayer" that is responsible for the transfer of shear between the constituents. The thickness of the interlayer is estimated from molecular dynamics study by approximating the distance between Van der Waals surfaces of two molecules. The details of steered molecular dynamics study in which the central collagen molecule is sheared with respect to the surrounding six other molecules, arranged in a quasihexagonal manner, can be found in our previous work [Pradhan et al. (2011)]. From the load-displacement response, the shear modulus and sliding/yield stress of the interlayer between collagen molecules are estimated to be  $0.07 \text{ pN}/\text{\AA}^2$  and  $0.166 \text{ pN}/\text{\AA}^2$  respectively. The shearing characteristic of collagen-mineral interface is studied by pulling collagen parallel to the mineral  $(10\bar{1}0)$  surface using steered molecular dynamics. The load-displacement response obtained from steered molecular dynamics is utilized to estimate shear modulus of interlayer using finite element method. This method allows us to separate the deformation of interlayer from that of collagen and mineral, during shearing. A finite element model of collagen pulled on the surface of the mineral is constructed using MSC Mentat, as shown in figure 1. This model consists of collagen and mineral separated by a 0.24 nm thick interlayer. The finite element simulation is carried out by fixing the bottom surface of the mineral and applying a load to the right end of collagen. A series of simulations were carried out by varying the shear modulus

of interlayer, until the stiffness response obtained matches the value obtained from steered molecular dynamics. The shear modulus of interlayer obtained from this iteration is  $1.51 \text{ pN}/\text{\AA}^2$ . The yield stress of the interlayer, when collagen pulled along the mineral surface, is estimated to be  $1.42 \text{ pN}/\text{\AA}^2$ . The elastic modulus and yield stress of hydroxyapatite, determined from nanoindentation test, obtained from the literature, are  $150.38 \text{ GPa}$  [Saber-Samandari and Gross (2009)] and  $2.42 \text{ GPa}$  respectively [Zamiri and De (2011)]. Both mineral and interlayer are modeled as elastic, perfectly-plastic material for finite element analysis.

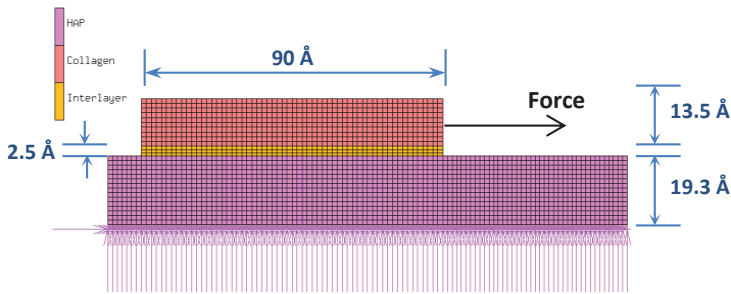


Figure 1: Finite element model of collagen pulled on the hydroxyapatite (HAP) mineral surface.



Figure 2: Section of the finite element model of collagen fibril showing banded pattern along the length formed by alternating gap and overlap zones.

The material properties of collagen and interlayers estimated from steered molecular dynamics are incorporated into the finite element model of collagen fibril. A finite element model of collagen fibril is constructed using MSC Mentat as described in detail in our previous work [Pradhan et al. (2014)]. This model of fibril is cylindrical in shape  $1005 \text{ nm}$  in length, approximately  $50 \text{ nm}$  in diameter, and consists of  $34$  molecules across the cross-sectional width. The total number of elements in this model are  $4,325,922$ , and the symmetric half of the model is used for simulation. The collagen molecules in this model are  $294.8 \text{ nm}$  long corresponding to  $4.4D$ , where  $D$  is the longitudinal stagger of  $67 \text{ nm}$ . The staggering of collagen

molecules with respect to each other in this model results in a banded pattern along the fibril length as shown in figure 2. The ends of collagen molecules consist of a region known a hole-zone that consists of a plate shaped hydroxyapatite 40 nm wide and 1.23 nm thick. The mineral plates in this model are aligned parallel to each other, with an arrangement similar to the parallel layers of hydroxyapatite seen in mineralized turkey tendon and some bones [Traub et al. (1989); Landis et al. (1993b); Landis et al. (1996); Weiner and Wagner (1998)]. The separation between adjacent collagen molecules in our model is 2.4 Å, which is taken from Landis et al. [Landis et al. (1993a)]. The crosslinks are modeled as the elements bridging the adjacent collagen molecules spanning 6 nm from the end of collagen molecules. The stiffness of crosslink is obtained from the literature [Buehler (2008)] with a value of 1181.143 pN/Å., while the bond strength of covalent crosslink is considered to be 2.1 nN [Grandbois et al. (1999); Lantz et al. (2001); Buehler (2006b)]. The simulations of collagen fibril were carried out for zero, one, two, three, four, and five crosslinks. The finite element simulations were carried out by fixing nodes on the bottom face and applying the fixed-displacement loadings to the nodes on the top face of the fibril model.

The values of parameters used for the development of crosslink model is presented in table 1.

### 3 Results and Discussion

The constituents of collagen fibril, the collagen molecule, mineral, and water, are known to have significant non-bonded interactions among themselves. The steered molecular dynamics studies show that the mechanical property of the collagen molecule is significantly affected by the mineral proximity. It has been shown in our previous work that the elastic modulus of the mineralized collagen fibril is significantly altered by the molecular interactions at the collagen-mineral interface [Pradhan et al. (2014)]. Here we study the effect of crosslink in the enhancement of mechanical property of collagen fibril due to the presence of mineral. The finite element simulations are carried out for crosslink densities varying from zero crosslink to five crosslinks per end of the collagen molecule. The elastic moduli of collagen fibril estimated at the small strain of 4% at various crosslink densities are shown in table 2. The table shows that the elastic modulus of collagen fibril at various crosslink densities is significantly higher when the influence of mineral on collagen mechanics is taken into consideration as compared to the case when the influence of mineral on collagen is not taken into account. Interestingly, the enhancement in the elastic modulus of fibril due to collagen-mineral interaction is found to exist irrespective of the presence of crosslink and exists at all crosslink densities!

Table 1: Parameters used in development of crosslink model.

Property	Value	Reference
Breaking stress at collagen and mineral detachment.	0.77 GPa (7.67 pN/Å <sup>2</sup> )	Obtained as described in section 2.1 in this work from the peak force during detachment of collagen and mineral.
The modulus of collagen pulled parallel to (10 $\bar{1}$ 0) and perpendicular to (0001) surfaces of hydroxyapatite.	13.17 and 6.26 GPa respectively.	Obtained in our previous work [Pradhan et al. (2014)]
The modulus of collagen pulled in absence of hydroxyapatite.	2.95 GPa	Obtained in our previous work [Pradhan et al. (2011)]
Shear modulus of interlayer between collagen and mineral	1.51 GPa (15.1 pN/Å <sup>2</sup> )	Obtained from iterations performed in this work as shown in section 2.2
Shear modulus of interlayer between collagen and collagen	0.007 GPa (0.07 pN/Å <sup>2</sup> )	Obtained in our previous work [Pradhan et al. (2011)]
Elastic modulus of hydroxyapatite	150.38 GPa	Obtained from nanoindentation from literature, [Saber-Samandari and Gross (2009)].
Stiffness of crosslinks	1181.143 pN/Å.	Obtained from the literature [Buehler (2008)]
Bond strength of covalent crosslink	2.1 nN	From Literature [Grandbois et al. (1999); Lantz et al. (2001); Buehler (2006b)].

Table 2: Elastic modulus of collagen fibril at various crosslink densities when the influence of hydroxyapatite on collagen mechanics is (i) taken into consideration, and (ii) not taken into consideration.

Number of Crosslinks	Elastic Modulus of Collagen Fibril (GPa)	
	(i) Mineral Influence	(ii) No Mineral Influence
0	3.99	3.52
3	4.33	3.79
5	4.43	3.89

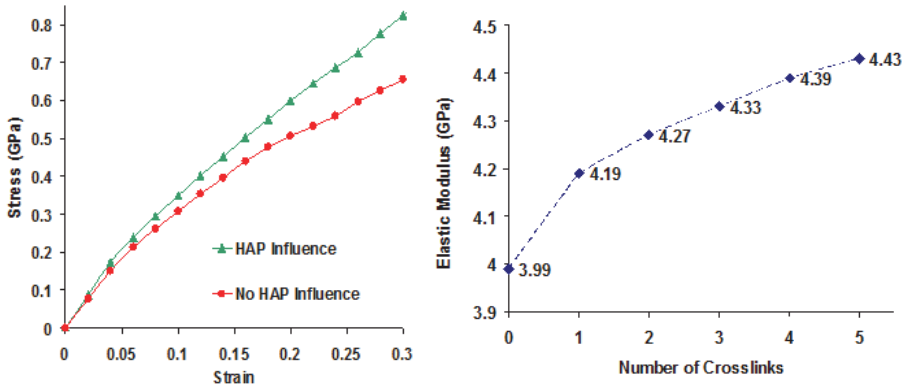


Figure 3: (a) Stress-strain response of collagen fibril when the influence of mineral proximity is taken into account and not taken into account. (b) Elastic modulus of collagen fibril at various crosslink densities.

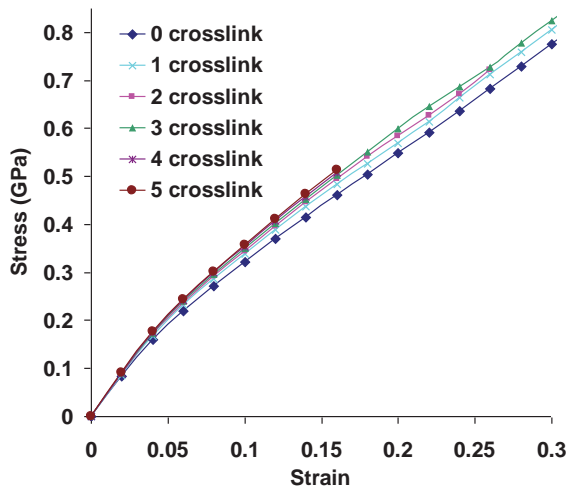


Figure 4: Stress-strain response of collagen fibril at crosslink densities varying from zero crosslink to five crosslinks per collagen end.

The typical stress-strain response of collagen fibril obtained from finite element simulation is shown in figure 3a. It is observed that, in addition to the small displacement regime, the deformation response of collagen fibril in the large displacement regime is significantly stiffer, when the effect of mineral proximity on collagen is taken into consideration. The simulations indicate that there is a significant enhancement in the stiffness response of collagen fibril in the large displacement

regime at all the crosslink densities.

The elastic modulus of collagen fibril corresponding to 4% strain at various crosslink densities is shown in figure 3b. It is seen in figure that the fibril exhibits higher elastic modulus at high crosslink densities. Furthermore, it is to be noted that there is a larger increment in elastic modulus between zero crosslink and one crosslink compared to between one, two, three, four, and five crosslinks. The enhancement in the elastic modulus due to the presence of crosslinks is seen to vary from 5% to 11% compared to the collagen fibril with no crosslink. This shows that the crosslinks play an important role in mechanics of collagen fibril by imparting higher elastic modulus.

The deformation response of collagen fibril at crosslink densities varying from zero crosslink to five crosslinks is shown in figure 4. It is seen from the plot that the larger number of crosslinks results in higher stiffness of collagen fibril.

A very interesting observation from this stress-strain response is that the yielding or failure of collagen fibril due to the breaking of crosslinks is not observed for any of the crosslink densities throughout the entire deformation range. A more striking observation from this plot is that the fibril model with no crosslink is also able to sustain the applied load without yielding or failure even at a large strain of 30%. In order to explain this observation, it is necessary to look closely at the arrangement of collagen molecules in a fibril. A schematic of the longitudinal section of collagen fibril approximately 1  $\mu\text{m}$  in length and 50 nm in diameter, consisting of 34 collagen molecules across the width, is shown in figure 5. The adjacent molecules are longitudinally staggered with respect to each other by 67 nanometers resulting in a gap and overlap zone of length 40 nanometers and 27 nanometers respectively along the length. Overlap zone is a region where the transfer of tensile force occurs between the adjacent collagen molecules with the help of crosslinks and shearing between molecules. Hence, pullout between the ends of collagen molecules in the overlap zone can be considered one of the important mechanisms of collagen fibril failure. As shown by the dotted lines in the figure, the adjacent overlap zones in collagen fibril are inclined at an angle of about 1.25 degrees relative to the longitudinal direction of fibril. The inclination of the lines can be estimated using a relation  $\text{Tan}^{-1}(d/D)$ , where  $d$  is a center-to-center lateral distance between collagen molecules and  $D$  is the D-spacing of 67 nanometers. Hence, the dotted lines represent the region where the collagen fibril fails due to the pullout between the overlapping ends of two molecules. While the pullout between the overlapping ends of two molecules is an important mechanism of fibril failure, it is essential to understand its dependency on the length and diameter of collagen fibril. Again referring to the schematic of collagen fibril shown in figure 5, a question arises as to, if it is possible to cause fibril to fail by pullout in the overlapping zone (i.e.

along the dotted lines), when the opposite ends of fibril are pulled? Considering a parallelogram shaped region of fibril bounded by two of the inclined dotted lines and red arrows on the left and right end of fibril section; evidently, there is no overlapping between the ends of collagen in this region, and hence the failure due to pullout and breaking of crosslinks is not possible. The deformation mechanism of this region is thus purely governed by the shearing between the adjacent collagen molecules. For the failure of collagen by pullout in the overlap zone to be possible, at least one of the dotted lines should intersect the opposite edges of fibril (i.e. top and bottom edges of a longitudinal section shown in figure 5). This gives rise to the concept of characteristic length ( $L_c$ ) of fibril that governs its deformation mechanism. The characteristic length is given by the relation,  $L_c = \phi \times D/d$ , where  $\phi$  is the diameter of fibril,  $D$  is the d-spacing of 67 nanometers, and  $d$  is a center-to-center lateral distance between collagen molecules. The deformation will be governed by intermolecular shear if the fibril length ( $L$ ) is shorter than  $L_c$ , whereas it will be governed by the pullout between collagen ends and breaking of crosslinks if  $L$  is longer than  $L_c$ . The diameter of collagen fibril model is  $50 \mu\text{m}$ , and its corresponding characteristic length is  $2.3 \mu\text{m}$ , which is much longer the length of the model (i.e.  $1 \mu\text{m}$ ). Due to this reason, yielding/failure of collagen fibril due to pullout between ends of collagen even when no crosslink is present (Fig. 4) is not observed. The fact that the mechanical response of collagen fibril is dependent on the size of fibril has also been shown experimentally. The experimental study by Shen et al. [Shen et al. (2008)] shows that the post yield behavior of collagen fibril is dependent on the fibril volume and as a result of which the collagen fibril cannot be considered by representative volume elements.

In bone, the exact mechanism of load transfer to fibrils is not very clear. There are currently two opposing viewpoints: (i) "load transfer to fibril occurs through proteoglycan bridges between fibrils" [Cribb and Scott (1995); Redaelli et al. (2003)], and (ii) "force transmission within the tissues occurs along spanning collagen fibrils themselves, long intertwined fibrils, and bifurcating/fusing fibrils" [Provenzano and Vanderby Jr (2006)]. Therefore, the true nature and distribution of the stress acting along the length of collagen fibril when the bone is strained is largely unknown. Further, it is not clear at this point whether, in bone, the load is most likely transferred to the collagen fibril as distributed stress acting along its length due to neighboring fibrils, or through interfibrillar mineral and proteoglycan bridges in different proportions. As a result, variable tensile stress is developed along the length of fibril with the presence of regions that are stressed and unstressed, i.e. every section along the length of fibril may not be under equal tensile strain and that there may be regions without any strain. Hence, we define the continuous length over which fibril experiences the tensile stress/strain due to the applied distributed load

as “effective length” for that particular loading condition, i.e. it is defined as the distance between two successive points of zero tension. The deformation mechanism of fibril depends on whether the effective length is greater or smaller than the characteristic length. If the effective length is greater than the characteristic length, the deformation mechanism is governed by the overlap zone and the breaking of crosslinks. However, if the effective length is less than the characteristic length, the deformation mechanism of fibril is governed by the intermolecular shear between collagen molecules. The finding that the deformation mechanism of collagen fibril is dependent on the characteristic length has an interesting implication for bone mechanics. As the characteristic length is directly proportional to the fibril diameter as discussed above, it can vary from the few  $\mu\text{m}$  for a fibril of small diameter to the tens of  $\mu\text{m}$  for a fibril of larger diameter. Because of this reason, fibrils of different diameter are likely to exhibit different deformation response for similar loading conditions.

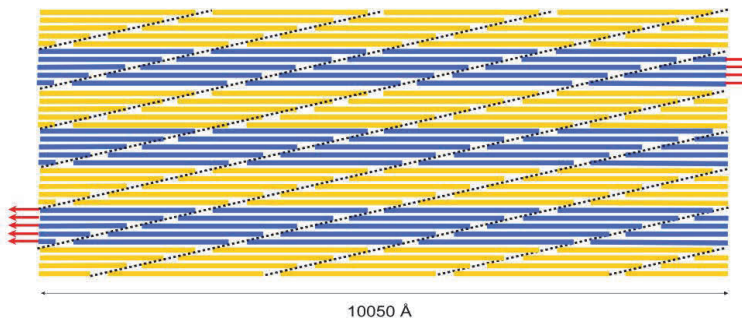


Figure 5: A schematic of the longitudinal section of collagen fibril in our model showing the arrangement of collagen molecules staggered with respect to each other by 67 nanometers. The dotted lines represent the location of the overlap zone where the crosslinks are formed near the end of the collagen molecule.

When the collagen fibril is stretched, the overlap and gap zone undergo different amounts of strain. The longitudinal strain along the collagen fibril in tension is shown in figure 6a. The gap zone undergoes significantly lesser strain compared to the overlap zone, as its deformation originates from the pure stretching of collagen molecules, nearly 50% of which are stiffened by the nonbonded interaction with hydroxyapatite due to the close proximity. Due to this reason, the collagen molecules in the overlap zone, which are closer to the mineral show lesser strain compared to the others. However, in the case of the overlap zone the deformation is achieved by shearing between the overlapping collagen molecules and the extension of crosslinks. In the overlap zone, the ends of collagen show lesser strain

compared to remaining length. The longitudinal stress along collagen fibril under tension is shown in figure 6b. The mineral component of fibril being very stiff experiences the highest magnitude of stress followed by the overlap zone. In the overlap zone, the region consisting of crosslinks experiences higher stress compared to the part that do not contain crosslinks. The strain energy per unit volume, stored in collagen fibril when it is stretched is shown in figure 6c. Overlap zone is the region that undergoes the highest strain, as a result of which the strain energy density is highest in this region.

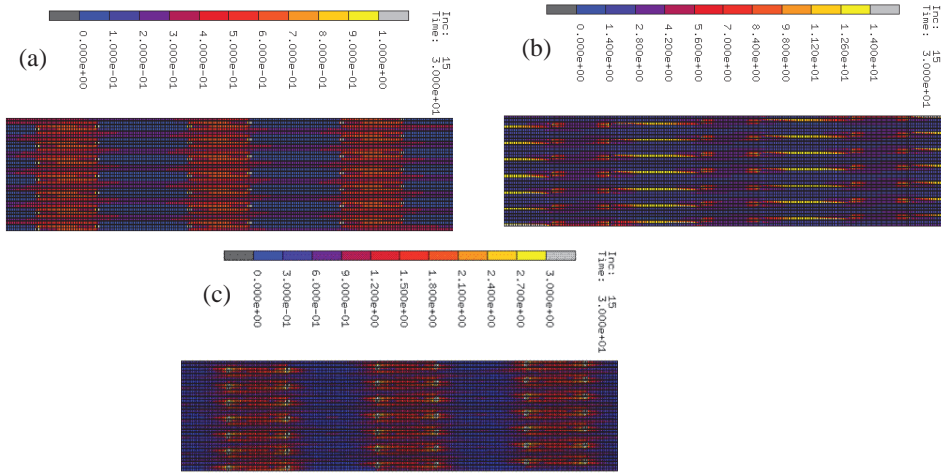


Figure 6: (a) Strain along collagen fibril in tension ( $\text{\AA}/\text{\AA}$ ). (b) Stress along collagen fibril in tension ( $\text{pN}/\text{\AA}^2$ ). (c) Strain energy density along collagen fibril in tension ( $\text{pN}\text{\AA} / \text{\AA}^3$ ).

#### 4 Conclusions

Multiscale modeling of collagen fibril is carried out by incorporating the material properties of collagen obtained from steered molecular dynamics into the finite element model of collagen fibril with the incorporation of crosslinks. The collagen fibril is extended using displacement control to evaluate its deformation response and the underlying mechanisms at various crosslink densities. The simulations indicate that the nonbonded interactions between collagen and mineral contribute to the significant enhancement of the elastic modulus of collagen fibril at all the crosslink densities, establishing the importance of taking into account these molecular interactions for modeling the mechanical response of collagen fibril. In addition to the

small displacement regime, the stiffening of collagen fibril due to molecular interactions between collagen and mineral is also observed in the large displacement regime of 30% strain. The crosslinks are found to play an important role in the mechanical response of collagen fibril, with enhancement in elastic modulus ranging from 5-11% for various crosslink densities compared to the elastic modulus of collagen fibril with no crosslinks. This stiffening behavior due to crosslinks is found to exist in small as well as large strain regimes, with the higher crosslink densities typically resulting in stiffer response of collagen fibril.

Further, in this study we have elucidated two different mechanisms of fibril deformation depending on the characteristic length of collagen fibril. The stress distribution within the collagen fibril affects the effective length for fibril deformation. The effective length is defined as the length of collagen fibril between two consecutive points of zero tension. The deformation mechanism is governed by the pullout between the ends of collagen molecules in the overlap zone, following the breaking of crosslinks, if the effective length is greater than the characteristic length. However, if the effective length is less than the characteristic length, the deformation mechanism is found to be dictated by the shearing between the staggered collagen molecules which are adjacent to each other. In this study, deformation response is found to be governed by the shearing between adjacent collagen molecules, as opposed to the pullout in the overlap region, since the effective length of our model is smaller than the characteristic length of fibril.

The overlap zone is seen to undergo higher strain compared to the gap zone. This is a result of the continuous length of collagen molecule present in the gap zone, enhancement of mechanical response of collagen due to nonbonded interactions with hydroxyapatite, as well as the additional stiffness provided by the mineral. The highest magnitude of stress is found in the mineral due to its high stiffness, followed by the overlap zone. In the overlap zone, the end regions consisting of crosslinks are found to experience higher stress compared to the non-crosslinked sections. Furthermore, the overlap zone due to its ability to undergo larger strain is found to have the higher concentration of strain energy compared to other regions of collagen fibril.

Hence, due to variation in length to diameter ratio of collagen fibrils in various tissues, fibrils of different diameters and same length or vice versa could exhibit different deformation response for similar loading conditions. Overall, this study elucidates the various nuances of the role of crosslinks on mechanics of collagen fibril while also incorporating the role of mineral proximity.

**Acknowledgement:** The authors acknowledge XCEDE supercomputing resources and NDSU Center for Computationally Assisted Science and Technology

(CCAST) for computational resources. Author S.M.P. acknowledges support from ND EPSCOR through a doctoral dissertation grant.

## References

- Almora-Barrios, N.; de Leeuw, N. H.** (2010): A Density Functional Theory Study of the Interaction of Collagen Peptides with Hydroxyapatite Surfaces. *Langmuir*, vol. 26, pp. 14535-14542.
- Bhattacharjee, A.; Bansal, M.** (2005): Collagen Structure: The Madras Triple Helix and the Current Scenario. *IUBMB Life*, vol. 57, pp. 161-172.
- Bhowmik, R.; Katti, K. S.; Katti, D.** (2007a): Molecular dynamics simulation of hydroxyapatite-polyacrylic acid interfaces. *Polymer*, vol. 48, pp. 664-674.
- Bhowmik, R.; Katti, K. S.; Katti, D. R.** (2007b): Mechanics of molecular collagen is influenced by hydroxyapatite in natural bone. *Journal of Materials Science*, vol. 42, pp. 8795-8803.
- Bhowmik, R.; Katti, K. S.; Katti, D. R.** (2009): Mechanisms of Load-Deformation Behavior of Molecular Collagen in Hydroxyapatite-Tropocollagen Molecular System: Steered Molecular Dynamics Study. *Journal of Engineering Mechanics-Asce*, vol. 135, pp. 413-421.
- Bozec, L.; Horton, M.** (2005): Topography and mechanical properties of single molecules of type I collagen using atomic force microscopy. *Biophysical Journal*, vol. pp. 88, 4223-4231.
- Buehler, M. J.** (2006a): Atomistic and continuum modeling of mechanical properties of collagen: elasticity, fracture, and self-assembly. *Journal of Materials Research*, vol. 21, pp. 1947-1961.
- Buehler, M. J.** (2006b): Nature designs tough collagen: Explaining the nanostructure of collagen fibrils. *Proceedings of the National Academy of Sciences of the United States of America*, vol. 103, pp. 12285-12290.
- Buehler, M. J.** (2007): Molecular nanomechanics of nascent bone: fibrillar toughening by mineralization. *Nanotechnology*, vol. 18.
- Buehler, M. J.** (2008): Nanomechanics of collagen fibrils under varying cross-link densities: Atomistic and continuum studies. *Journal of the Mechanical Behavior of Biomedical Materials*, vol. 1, pp. 59-67.
- Cribb, A. M.; Scott, J. E.** (1995): Tendon response to tensile stress: an ultrastructural investigation of collagen: proteoglycan interactions in stressed tendon. *Journal of anatomy*, vol. 187.
- Currey, J. D.** (1990): Biomechanics of mineralized skeletons. In: Carter JG (ed): Skeletal Biomineralization :Patterns, processes, and evolutionary trends, 1 edn. Van

*Nostrand, New York.* pp. 11.

**Currey, J. D.; Zioupos, P.; Davies, P.; Casinos, A.** (2001): Mechanical properties of nacre and highly mineralized bone. *Proceedings of the Royal Society of London Series B-Biological Sciences*, vol. 268, pp. 107-111.

**Dorozhkin, S. V.; Epple, M.** (2002): Biological and medical significance of calcium phosphates. *Angewandte Chemie, International Edition*, vol. 41, pp. 3130-3146.

**Dubey, D. K.; Tomar, V.** (2009a): Role of hydroxyapatite crystal shape in nanoscale mechanical behavior of model tropocollagen-hydroxyapatite hard biomaterials. *Materials Science and Engineering: C*, vol. 29, pp. 2133-2140.

**Dubey, D. K.; Tomar, V.** (2009b): Role of the nanoscale interfacial arrangement in mechanical strength of tropocollagen-hydroxyapatite-based hard biomaterials. *Acta Biomaterialia*, vol. 5, pp. 2704-2716.

**Dubey, D. K.; Tomar, V.** (2010): Effect of changes in tropocollagen residue sequence and hydroxyapatite mineral texture on the strength of ideal nanoscale tropocollagen-hydroxyapatite biomaterials. *Journal of Materials Science-Materials in Medicine*, vol. 21, pp. 161-171.

**Eastoe, J. E.; Eastoe, B.** (1954): Organic constituents of mammalian compact bone. *Biochemical Journal*, vol. 57, pp. 453-459.

**Feller, S. E.; Zhang, Y. H.; Pastor, R. W.; Brooks, B. R.** (1995): CONSTANT-PRESSURE MOLECULAR-DYNAMICS SIMULATION - THE LANGEVIN PISTON METHOD. *Journal of Chemical Physics*, vol. 103, pp. 4613-4621.

**Fisher, L. W.; Termine, J. D.** (1985): Noncollagenous proteins influencing the local mechanisms of calcification. *Clinical Orthopaedics and Related Research*, vol. 200, pp. 362-385.

**Fratzl, P.; Weinkamer, R.** (2007): Nature's hierarchical materials. *Progress in Materials Science*, vol. 52, pp. 1263-1334.

**Fritsch, A.; Hellmich, C.; Dormieux, L.** (2009): Ductile sliding between mineral crystals followed by rupture of collagen crosslinks: Experimentally supported micromechanical explanation of bone strength. *Journal of Theoretical Biology*, vol. 260, pp. 230-252.

**Gautieri, A.; Buehler, M. J.; Redaelli, A.** (2009): Deformation rate controls elasticity and unfolding pathway of single tropocollagen molecules. *Journal of the Mechanical Behavior of Biomedical Materials*, vol. 2, pp. 130-137.

**Gautieri, A.; Vesentini, S.; Redaelli, A.; Buehler, M. J.** (2011): Hierarchical Structure and Nanomechanics of Collagen Microfibrils from the Atomistic Scale Up. *Nano Letters*, vol. 11, pp. 757-766.

- Ghosh, P.; Katti, D. R.; Katti, K. S.** (2007): Mineral Proximity Influences Mechanical Response of Proteins in Biological Mineral-Protein Hybrid Systems. *Biomacromolecules*, vol. 8, pp. 851-856.
- Grandbois, M.; Beyer, M.; Rief, M.; Clausen-Schaumann, H.; Gaub, H. E.** (1999): How Strong Is a Covalent Bond? *Science*, vol. 283, pp. 1727.
- Gupta, H. S.; Wagermaier, W.; Zickler, G. A.; Hartmann, J.; Funari, S. S.; Roschger, P.; Wagner, H. D.; Fratzl, P.** (2006): Fibrillar level fracture in bone beyond the yield point. *International Journal of Fracture*, vol. 139, pp. 425-436.
- Hellmich, C.; Barthelemy, J. F.; Dormieux, L.** (2004): Mineral-collagen interactions in elasticity of bone ultrastructure - a continuum micromechanics approach. *European Journal of Mechanics a-Solids*, vol. 23, pp. 783-810.
- Hodge, A. J.; Petruska, J. A.** (1963): Recent studies with the electron microscope on ordered aggregates of the tropocollagen molecule. In: Ramachandran GN (ed) Aspects of Protein Structure. *Academic Press, New York*. pp. 289-300.
- Hulmes, D. J.; Wess, T. J.; Prockop, D. J.; Fratzl, P.** (1995): Radial packing, order, and disorder in collagen fibrils. *Biophysical Journal*, vol. 68, pp. 1661-1670.
- Hulmes, D. J. S.** (2002) Building collagen molecules, fibrils, and suprafibrillar structures. *Journal of Structural Biology*, vol. 137, pp. 2-10.
- Kadler, K. E.; Holmes, D. F.; Trotter, J. A.; Chapman, J. A.** (1996): Collagen fibril formation. *Biochemical Journal*, vol. 316, pp. 1-11.
- Katti, D. R.; Pradhan, S. M.; Katti, K. S.** (2010): Directional dependence of hydroxyapatite-collagen interactions on mechanics of collagen. *Journal of Biomechanics*, vol. 43, pp. 1723-1730.
- Katti, K. S.; Katti, D. R.; Tang, J.; Pradhan, S.; Sarikaya, M.** (2005): Modeling mechanical responses in a laminated biocomposite - Part II - Nonlinear responses and nuances of nanostructure. *Journal of Materials Science*, vol. 40, pp. 1749-1755.
- Koch, M.; Laub, F.; Zhou, P.; Hahn, R. A.; Tanaka, S.; Burgeson, R. E.; Gerecke, D. R.; Ramirez, F.; Gordon, M. K.** (2003): Collagen XXIV, a Vertebrate Fibrillar Collagen with Structural Features of Invertebrate Collagens. *Journal of Biological Chemistry*, vol. 278, pp. 43236-43244.
- Landis, W. J.** (1995): The strength of a calcified tissue depends in part on the molecular structure and organization of its constituent mineral crystals in their organic matrix. *Bone (New York, NY, United States)*, vol. 16, pp. 533-544.
- Landis, W. J.; Hodgens, K. J.; Song, M. J.; Arena, J.; Kiyonaga, S.; Marko, M.; Owen, C.; McEwen, B. F.** (1996): Mineralization of collagen may occur on

fibril surfaces: evidence from conventional and high-voltage electron microscopy and three-dimensional imaging. *Journal of structural biology*, vol. 117, pp. 24-35.

**Landis, W. J.; Song, M. J.; Leith, A.; McEwen, L.; McEwen, B. F.** (1993a): Mineral and Organic Matrix Interaction in Normally Calcifying Tendon Visualized in 3 Dimensions by High-Voltage Electron-Microscopic Tomography and Graphic Image-Reconstruction. *Journal of Structural Biology*, vol. 110, pp. 39-54.

**Landis, W. J.; Song, M. J.; Leith, A.; McEwen, L.; McEwen, B. F.** (1993b): Mineral and organic matrix interaction in normally calcifying tendon visualized in three dimensions by high-voltage electron microscopic tomography and graphic image reconstruction. *Journal of structural biology*, vol. 110, pp. 39-54.

**Lantz, M. A.; Hug, H. J.; Hoffmann, R.; van Schendel, P. J. A.; Kappenberger, P.; Martin, S.; Baratoff, A.; Güntherodt, H. J.** (2001): Quantitative Measurement of Short-Range Chemical Bonding Forces. *Science*, vol. 291, pp. 2580-2583.

**Lorenzo, A. C.; Caffarena, E. R.** (2005): Elastic properties, Young's modulus determination and structural stability of the tropocollagen molecule: a computational study by steered molecular dynamics. *Journal of Biomechanics*, vol. 38, pp. 1527-1533.

**MacKerell, A. D.; Bashford, D.; Bellott, M.; Dunbrack, R. L.; Evanseck, J. D.; Field, M. J.; Fischer, S.; Gao, J.; Guo, H.; Ha, S.; Joseph-McCarthy, D.; Kuchnir, L.; Kuczera, K.; Lau, F. T. K.; Mattos, C.; Michnick, S.; Ngo, T.; Nguyen, D. T.; Prodhom, B.; Reiher, W. E.; Roux, B.; Schlenkrich, M.; Smith, J. C.; Stote, R.; Straub, J.; Watanabe, M.; Wiorkiewicz-Kuczera, J.; Yin, D.; Karplus, M.** (1998): All-atom empirical potential for molecular modeling and dynamics studies of proteins. *Journal of Physical Chemistry B*, vol. 102, pp. 3586-3616.

**Moradianoldak, J.; Weiner, S.; Addadi, L.; Landis, W. J.; Traub, W.** (1991): Electron Imaging and Diffraction Study of Individual Crystals of Bone, Mineralized Tendon and Synthetic Carbonate Apatite. *Connective Tissue Research*, vol. 25, pp. 219-228.

**Nanci, A.** (1999): Content and distribution of noncollagenous matrix proteins in bone and cementum: relationship to speed of formation and collagen packing density. *Journal of structural biology*, vol. 126, pp. 256-269.

**Nylen, M. U.; Scott, D. B.; Mosley, V. M.** (1960): Mineralization of turkey leg tendon. II. Collagen-mineral relations revealed by electron and x-ray microscopy. No. 64, pp. 129-142.

**Olszta, M. J.; Odom, D. J.; Douglas, E. P.; Gower, L. B.** (2003): A New Paradigm for Biomineral Formation: Mineralization via an Amorphous Liquid-Phase Precursor. *Connective Tissue Research*, vol. 44, pp. 326-334.

**Pace, J. M.; Corrado, M.; Missero, C.; Byers, P. H.** (2003): Identification, characterization and expression analysis of a new fibrillar collagen gene, COL27A1. *Matrix Biology*, vol. 22, pp. 3-14.

**Phillips, J. C.; Braun, R.; Wang, W.; Gumbart, J.; Tajkhorshid, E.; Villa, E.; Chipot, C.; Skeel, R. D.; Kale, L.; Schulten, K.** (2005): Scalable molecular dynamics with NAMD. *Journal of Computational Chemistry*, vol. 26, pp. 1781-1802.

**Pradhan, S.; Katti, K.; Katti, D.** (2014): A Multiscale Model of Collagen Fibril in Bone: Elastic Response. *Journal of Engineering Mechanics*, vol.140, No. 3, pp.454-461.

**Pradhan, S. M.; Katti, D. R.; Katti, K. S.** (2011): Steered Molecular Dynamics Study of Mechanical Response of Full Length and Short Collagen Molecules. *Journal of Nanomechanics and Micromechanics*, vol. 1, pp. 104-110.

**Provenzano, P. P.; Vanderby, Jr. R.** (2006): Collagen fibril morphology and organization: Implications for force transmission in ligament and tendon. *Matrix Biology*, vol. 25; pp. 71-84.

**Qin, Z.; Gautieri, A.; Nair, A. K.; Inbar, H.; Buehler, M. J.** (2012): Thickness of Hydroxyapatite Nanocrystal Controls Mechanical Properties of the Collagen-Hydroxyapatite Interface. *Langmuir*, vol. 28, pp. 1982-1992.

**Ramachandran, G. N.; Kartha, G.** (1955): Structure of Collagen. *Nature*, vol. 176, pp. 593-595.

**Redaelli, A.; Vesentini, S.; Soncini, M.; Vena, P.; Mantero S.; Montevecchi, F. M.** (2003): Possible role of decorin glycosaminoglycans in fibril to fibril force transfer in relative mature tendons—a computational study from molecular to microstructural level. *Journal of Biomechanics*, vol. 36, pp. 1555-1569.

**Saber-Samandari, S.; Gross, K. A.** (2009): Micromechanical properties of single crystal hydroxyapatite by nanoindentation. *Acta Biomaterialia*, vol. 5, pp. 2206-2212.

**Shen, Z. L.; Dodge, M. R.; Kahn, H.; Ballarini, R.; Eppell, S. J.** (2008): Stress-strain experiments on individual collagen fibrils. *Biophysical Journal*, vol. 95, pp. 3956-3963.

**Sikdar, D.; Pradhan, S. M.; Katti, D. R.; Katti, K. S.; Mohanty, B.** (2008): Altered phase model for polymer clay nanocomposites. *Langmuir*, vol. 24, pp. 5599-5607.

**Streeter, I.; de Leeuw, N. H.** (2010): Atomistic Modeling of Collagen Proteins in Their Fibrillar Environment. *Journal of Physical Chemistry B*, vol. 114, pp. 13263-13270.

**Streeter, I.; de Leeuw, N. H.** (2011): A molecular dynamics study of the interprotein interactions in collagen fibrils. *Soft Matter*, vol. 7, pp. 3373-3382.

**Tang, Y.; Ballarini, R.; Buehler, M. J.; Eppell, S. J.** (2010): Deformation micromechanisms of collagen fibrils under uniaxial tension. *Journal of The Royal Society Interface*, vol. 7, pp. 839-850.

**Termine, J. D.; Robey, P. G.** (1996): Bone matrix proteins and the mineralization process. In: Favus MJ (ed) Primer on the Metabolic Bone Diseases and Disorders of Mineral Metabolism. *The American Society for Bone and Mineral Research, Lippincott Williams & Wilkins*. Third edition, pp. 24-28.

**Traub, W.; Arad, T.; Weiner, S.** (1989): Three-dimensional ordered distribution of crystals in turkey tendon collagen fibers. *Proceedings of the National Academy of Sciences of the United States of America*, vol. 86, pp. 9822-9826.

**Weiner, S.; Wagner, H. D.** (1998): The material bone: structure-mechanical function relations. *Annual Review of Materials Science*, vol. 28, pp. 271-298.

**Zamiri, A.; De, S.** (2011): Mechanical properties of hydroxyapatite single crystals from nanoindentation data. *Journal of the Mechanical Behavior of Biological Materials*, vol. 4, pp. 146-152.

